Thermodynamics of Small Alkali Metal Halide Cluster Ions: Comparison of Classical Molecular Simulations with Experiment and Quantum Chemistry

ARTICLE *in* THE JOURNAL OF PHYSICAL CHEMISTRY A · DECEMBER 2014

Impact Factor: 2.69 · DOI: 10.1021/jp509401d · Source: PubMed

5 AUTHORS, INCLUDING:

Lukas Vlcek
Oak Ridge National Laboratory
67 PUBLICATIONS **682** CITATIONS
SEE PROFILE

Filip Moučka
Jan Evangelista Purkyně University
27 PUBLICATIONS **231** CITATIONS
SEE PROFILE

Ivo Nezbeda
Academy of Sciences of the Czech Republic
237 PUBLICATIONS **3,553** CITATIONS
SEE PROFILE

THE JOURNAL OF PHYSICAL CHEMISTRY A

Article

pubs.acs.org/JPCA

Thermodynamics of Small Alkali Metal Halide Cluster Ions: Comparison of Classical Molecular Simulations with Experiment and Quantum Chemistry

Lukas Vlcek,*[,†,‡] Filip Uhlik,[§] Filip Moucka,[∥] Ivo Nezbeda,[∥,⊥] and Ariel A. Chialvo[†]

[†]Chemical Sciences Division, Geochemistry & Interfacial Sciences Group, Oak Ridge National Laboratory, Oak Ridge, Tennessee 37831-6110, United States

[‡]Joint Institute for Computational Sciences, Oak Ridge National Laboratory, Oak Ridge, Tennessee 37831-6173, United States

[§]Department of Physical and Macromolecular Chemistry, Faculty of Science, Charles University, 128 43 Prague 2, Czech Republic

[∥]Faculty of Science, J. E. Purkinje University, 400 96 Usti nad Labem, Czech Republic

[⊥]E. Hala Laboratory of Thermodynamics, Institute of Chemical Process Fundamentals, Academy of Sciences, 165 02 Prague 6, Czech Republic

Supporting Information

ABSTRACT: We evaluate the ability of selected classical molecular models to describe the thermodynamic and structural aspects of gas-phase hydration of alkali metal halide ions and the formation of small water clusters. To understand the effect of many-body interactions (polarization) and charge penetration effects on the accuracy of a force field, we perform Monte Carlo simulations with three rigid water models using different functional forms to account for these effects: (i) point charge nonpolarizable SPC/E, (ii) Drude point charge polarizable SWM4-DP, and (iii) Drude Gaussian charge polarizable BK3. Model predictions are compared with experimental Gibbs free energies and enthalpies of ion hydration, and with microscopic structural properties obtained from quantum DFT calculations. We find that all three models provide comparable predictions for pure water clusters and cation hydration but differ significantly in their description of anion hydration. None of the investigated classical force fields can consistently and quantitatively reproduce the experimental gas-phase hydration thermodynamics. The outcome of this study highlights the relation between the functional form that describes the effective intermolecular interactions and the accuracy of the resulting ion hydration properties.

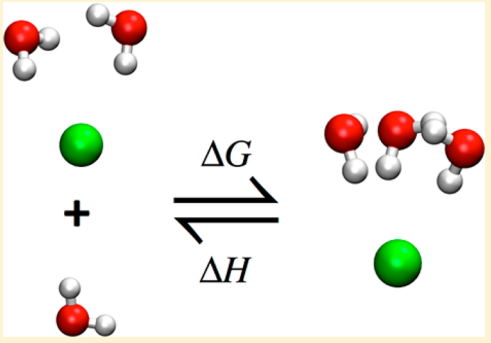

1. INTRODUCTION

An accurate representation of ion hydration at low water densities is critical for the study of diverse atmospheric processes, such as cluster and droplet formation in the ionosphere,[1] seawater sprays,[2] flames,[3,4] or electric discharges,[5] as well as for understanding the behavior of aqueous electrolytes in supercritical geochemical and industrial systems.[6,7] Beyond specific applications, small vapor-phase cluster ions offer a unique window into the fundamental problem of single-ion solvation thermodynamics because, unlike ions in bulk liquid solutions, individual cluster properties can be studied experimentally using mass spectrometric methods based on equilibrium measurements[8−14] and collision-induced dissociation.[15−17] The experimental results have been used as anchoring points for the extrapolation of hydration properties to bulk conditions,[18,19] as well as for the development and validation of classical molecular force fields.[20−25] The small size of cluster ions, typically comprising less than 10 water molecules, also provides a more direct insight into the specific details of ion−water interactions than bulk aqueous systems, which makes these systems a valuable source of information for force field optimization.

Computational studies of small gas-phase clusters have traditionally relied heavily on first-principles quantum chemical approaches. Given the limited system sizes, accurate high-level quantum methods can be used to calculate the energies of selected cluster configurations[24] and lower-level DFT calculations can be used to collect samples from the first-principles molecular dynamics (MD) or Monte Carlo (MC) simulations at finite temperatures.[26,27] At present, such simulations routinely cover MD trajectories spanning tens of picoseconds or generate thousands of MC cycles, which is sufficient for basic estimation of the cluster thermodynamics.[27] However, because accurate determination of thermodynamic properties (e.g., Gibbs free energy and entropy of hydration) requires much more extensive sampling of the system phase-space in the order

Received: September 17, 2014
Revised: November 16, 2014
Published: December 16, 2014

DOI: 10.1021/jp509401d
J. Phys. Chem. A 2015, 119, 488−500

of tens of nanoseconds, which is not currently achievable by straightforward DFT-MD simulations, such calculations must be accomplished by either classical simulations or quantum/classical hybrid schemes.

Classical simulations of cluster ions have been used both to develop molecular models and to study ion hydration in vapor phases.[20−25] Perhaps the most common way cluster ions are used in force field development is as a reference for adjustment of interaction parameters to reproduce *ab initio* polymerization energies of selected locally optimized configurations. This approach, typically employed for polarizable models,[28−35] has also been used by Joung and Cheatham to develop their alkali metal halide force fields compatible with nonpolarizable models of water.[23] Although methodologically simple, the optimization based on minimum energy configurations may suffer from a bias resulting from overweighting more compact structures while underweighting a wide range of higher-energy structures that can contribute significantly to the cluster hydration entropy. This bias, however, can be avoided by using a larger number of canonically distributed cluster configurations obtained from MD or MC simulations at finite temperatures (usually at 298.15 K), whereas the model parameters can be then adjusted to reproduce experimental thermodynamic properties, trajectories from DFT-MD simulations, or both. This approach was used by Smith and Dang, who optimized their ion force-field parameters compatible with the polarizable water model (RPOL) to match incremental hydration enthalpies of Na^+ and Cl^- ions.[36] Likewise, Lamoreux and Roux adjusted the ion−water parameters on the basis of their SWM4-DP model to reproduce the empirical enthalpies of ion monohydrates and found that the resulting model was able to predict reasonably well selected *ab initio* energies of larger clusters.[24] Moreover, Shevkunov used experimental cluster-ion thermodynamic properties to design a nonpolarizable force field specifically for the description of Cl^-−water clusters,[37] whereas Lukyanov et al. performed an extensive systematic evaluation of the capability of a set of simple polarizable and nonpolarizable models to predict cluster-ion binding hydration Gibbs free energies, enthalpies, and entropies,[20] whose analysis has been recently extended by Zidi using a fluctuating charge polarizable model.[38] Finally, Grossfield et al. calculated the Cl^- cluster binding enthalpies for the flexible polarizable AMOEBA force field and found a close agreement with the high pressure mass spectrometry counterpart.[33]

Though there have been numerous studies of small and medium size ion−water clusters addressing different challenges of the molecular based interpretation of ion hydration phenomena,[38−41] there is also an underlying interest in developing an accurate representation of ion−water clusters motivated by their key role in the determination of single-ion hydration properties.[18,42,43] However, as argued in our recent study with nonpolarizable models[19] and later supported by simulations with the more sophisticated polarizable AMOEBA model,[44] the current extrapolations from clusters to bulk hydration rely on unjustified assumptions. A direct path to more accurate determination of single-ion thermodynamics is to span the experimentally inaccessible cluster-to-bulk transition using highly accurate molecular models. In the present study we investigate the ability of three currently available classical rigid models (and corresponding force field parametrizations) to describe the properties of small ion−water clusters as determined by macroscopic thermodynamic experiments and microscopic quantum mechanical simulations. These models are characterized by contrasting approaches used to account for polarization effects that range from pairwise effective polarizable contributions using fixed-charge electrostatics, to multibody induced polarization via molecular Drude point charges (one per H_2O),[24] and finally to polarization described by atomic Drude oscillators with Gaussian charges (three per H_2O).[28] The analysis of model behavior across large data sets can reveal trends that would not be apparent from isolated data points and identify essential interactions needed for reliable description of ion hydration. The outcome of this comparison should provide guidance for future development of highly accurate potential models to facilitate large-scale simulations of aqueous ions in both vapor and liquid phases over a wide range of thermodynamic conditions and environments. Even though we employ a simple flexible model of water in our hybrid classical-quantum DFT Monte Carlo scheme, we defer a more comprehensive analysis of the role of flexibility and other features to future studies.

The remainder of the article is organized as follows: In section 2 we define the essential concepts and models needed for the study of cluster ions and describe our computational methodology; in section 3 we present structural and thermodynamic results pertaining to cluster-ions and discuss the performance of different force fields; in section 4 we summarize our findings and highlight their implications in the development of more accurate aqueous electrolyte interaction models.

2. THEORETICAL BACKGROUND

2.1. Basic Relations. The thermodynamics of gas-phase ion hydration and formation of cluster ions at finite temperatures and pressures is typically expressed in terms of elementary stepwise (or incremental) reactions and their associated enthalpies and Gibbs free energies.

The standard state (i.e., T° = 298.15 K and P° = 1 bar) enthalpy, $\Delta H^\circ_{n-1,n}[A]$, and Gibbs free energy, $\Delta G^\circ_{n-1,n}[A]$, of the stepwise hydration reaction

$$A(H_2O)_{n-1} + H_2O \rightarrow A(H_2O)_n \tag{1}$$

in which a cluster ion comprising an ion A and $n - 1$ water molecules binds an additional water molecule, can be expressed as follows,

$$\Delta H^\circ_{n-1,n}[A] = H^\circ[A(H_2O)_n] - H^\circ[A(H_2O)_{n-1}] - H^\circ[H_2O] \tag{2a}$$

$$\Delta G^\circ_{n-1,n}[A] = G^\circ[A(H_2O)_n] - G^\circ[A(H_2O)_{n-1}] - G^\circ[H_2O] \tag{2b}$$

The thermodynamic quantities listed on the right-hand side of eqs 2 correspond to individual reactants and products (i.e., cluster ions comprising n and $n - 1$ water molecules, and a single water molecule, respectively) in the ideal gas state at standard conditions. The enthalpies of reactants and products appearing in eq 2a can be decomposed into the following components,

$$H^\circ = K^\circ + U + P^\circ V \tag{3}$$

where K° and U are the average kinetic and potential energies and V is the molar volume of the species at the standard pressure P°. Because the interparticle potential energy of an isolated water molecule is zero, it results that, to determine $\Delta H^\circ_{n-1,n}[A]$, it suffices to calculate the difference between the enthalpies of cluster ions comprising n and $n - 1$ water

DOI: 10.1021/jp509401d
J. Phys. Chem. A 2015, 119, 488−500

molecules followed by the subtraction of the ideal gas enthalpy contribution of classical rigid water molecules ($3RT$ for translational and rotational degrees of freedom and $1RT$ for the PV term of ideal gas) at the standard temperature T°, i.e.,

$$\Delta H^\circ_{n-1,n}[\mathrm{A}] = H^\circ[\mathrm{A(H_2O)}_n] - H^\circ[\mathrm{A(H_2O)}_{n-1}] - 4RT^\circ \quad (4)$$

The difference of Gibbs free energy between clusters comprising n and $n-1$ water molecules, i.e., the first two terms in the right-hand side of eq 2b, can be extracted from the grand canonical probability $p_i(n)$ of finding a cluster-ion with n water molecules in a system characterized by the chemical potential of water, $\mu_i(T,V)$, defined as

$$p_i(n) = \frac{Q(n)\exp[\beta\mu_i n]}{\exp[-\beta\Omega_i]} \quad (5)$$

where Ω_i is the classical bulk grand potential ($\Omega_i = -P_iV$) and $Q(n)$ is the canonical partition function of a system with one ion and n water molecules within volume V, at temperature T, where $\beta = 1/k_BT$, and k_B is the Boltzmann constant. The probability $p_i(n)$ can be calculated using grand canonical Monte Carlo (GCMC) simulations from a normalized histogram,

$$p_i(n) = \frac{\mathcal{H}_i(n)}{\mathcal{H}_i^{\mathrm{TOT}}} \quad (6)$$

where $\mathcal{H}_i(n)$ denotes the histogram count for clusters with n water molecules and $\mathcal{H}_i^{\mathrm{TOT}}$ is the total number of cluster-size measurements. Because the ideal gas $P^\circ V$ contributions from the two cluster ions cancel out, the difference of Gibbs free energies in eq 2b can be equated to the corresponding difference of Helmholtz free energies $\Delta F(n,n-1)$ which, according to eqs 5 and 6, can be expressed as

$$\beta\{F[\mathrm{A(H_2O)}_n] - F[\mathrm{A(H_2O)}_{n-1}]\} = -\ln\left[\frac{Q(n)}{Q(n-1)}\right] = -\ln\left[\frac{\mathcal{H}_i(n)}{\mathcal{H}_i(n-1)}\right] + \beta\mu_i \quad (7)$$

Equation 7 suggests that, from a simulation standpoint, a series of GCMC simulations of clusters at different values of $\mu_i(T,V)$ can be seamlessly combined using the histogram reweighting technique.[19,45] Subsequently, the stepwise Gibbs free energy difference defined in eq 2b can be finally calculated as follows,

$$\Delta G^\circ_{n-1,n}[\mathrm{A}] = F[\mathrm{A(H_2O)}_n] - F[\mathrm{A(H_2O)}_{n-1}] - \mu^{\circ,\mathrm{ig}}[\mathrm{H_2O}] \quad (8)$$

where $\mu^{\circ,\mathrm{ig}}[\mathrm{H_2O}]$ is the chemical potential of isolated (ideal gas) water molecules at the standard conditions (P°, T°).

In the case of small pure-water clusters, whose instability results in poor GCMC sampling, the free energy difference between clusters composed of n and $n-1$ water molecules, $\Delta F(n,n-1)$, can be determined more efficiently using Bennett's acceptance ratio (BAR) method,[46] which permits a more flexible and focused sampling of the configurational space. To apply this approach to the hydration reaction of eq 1, the reaction path must be split into two steps: (i) add a noninteracting water molecule to a cluster with $n-1$ water molecules, followed by (ii) switch on the interactions of the new molecule with the rest of the system, i.e.,

$$\beta\{F[\mathrm{A(H_2O)}_n] - F[\mathrm{A(H_2O)}_{n-1}]\} = -\ln\left[\frac{Q_0(n)}{Q(n-1)}\right] - \ln\left[\frac{Q(n)}{Q_0(n)}\right] \quad (9)$$

where $Q_0(n)$ denotes the canonical partition function of a cluster ion with one noninteracting and $n-1$ interacting water molecules. The first term on the right-hand side of eq 9 corresponds to the Helmholtz free energy of a noninteracting water molecule moving within the volume of a cluster comprising n water molecules, i.e.,

$$\frac{Q_0(n)}{Q(n-1)} = \frac{V}{nq^{\mathrm{iso}}} \quad (10)$$

where q^{iso} stands for the product of the translational, rotational, vibrational, and electronic partition functions of an isolated water molecule.[47] The second term on the right-hand side of eq 9 corresponds to the free energy change caused by switching on the interactions of the extra particle. The magnitude of this contribution can be determined using Widom's test particle method[48] with canonical MC or MD simulations of a cluster with $n-1$ water molecules, i.e.,

$$\frac{Q(n)}{Q_0(n)} = \langle\exp[-\beta(u-u_0)]\rangle_0 \quad (11)$$

Here u and u_0 are the energies of the same configuration in the systems with n and $n-1$ fully interacting water molecules and $\langle\ldots\rangle_0$ denotes averaging over equilibrium configurations of the system with one noninteracting molecule. However, to reduce any bias that can be introduced by the test particle method when extensive sampling is not available, we use the BAR method, which combines samples taken from the two systems characterized by $Q(n)$ and $Q_0(n)$, i.e.,

$$\frac{Q(n)}{Q_0(n)} = \frac{\langle w\exp[-\beta u]\rangle_0}{\langle w\exp[-\beta u_0]\rangle} \quad (12)$$

where w is a properly chosen weighting function.[46] Because the noninteracting particle can easily sample configurations present in the fully interacting system, there is enough overlap between configurations of $Q(n)$ and $Q_0(n)$, and the outcome of eq 12 should not be significantly biased. The variance (i.e., as a measure of the statistical error) of the calculated free energy averages can be reduced by a judicious adjustment of the relative number of samples taken from the two systems. As a test of correctness of our BAR and GCMC implementations, we have confirmed that both methods yield the same cluster-ion $\Delta F(n,n-1)$ values.

2.2. Definition of a Cluster. The analysis of cluster-ion properties and their comparison with the corresponding experimental data requires a definition of what constitutes a cluster that is compatible with the experimental setup. Because most ion−water and water−water clusters at finite temperatures are transient structures, any criterion used for their definition must select structures stable enough to undergo the experimental measurement.

Perhaps the most sophisticated cluster definitions are based on kinetic considerations of cluster stability derived from the rate of evaporation, which have been used to study a water dimer.[49] Unfortunately, this approach is not practical for the present study that involves millions of possible configurations of up to 7 particles. Other definitions involve geometrical

DOI: 10.1021/jp509401d
J. Phys. Chem. A 2015, 119, 488−500

criteria based on particle-pair connectivity,[50] as well as distance-based criteria specifically designed to deal with cluster ions.[51] Though simple in specific cases, geometrical criteria are difficult to generalize for more complex systems containing mixtures of molecular particles, such as in the present study, which requires consistent treatment of cluster ions and pure water clusters. Instead, here we opt for two energy-based stability criteria, A and B, similar to those proposed by Hill[52,53] and used for simple and fast identification of clusters.[54,55] Neither of our criteria will result in the selection of indefinitely stable clusters, with the exception of a dimer of structureless atomic particles. According to criterion A, a stable dimer is formed when the pair interaction energy is lower than the mutual kinetic energy, i.e.,

$$u_{ij}(\mathbf{r}_i,\mathbf{r}_j) \le -(\mathbf{p}_i - \mathbf{p}_j)^2/4\mu \tag{13}$$

Here i and j represent two particles or groups of particles whose mutual interaction energy is u_{ij}, $\mathbf{r}_i$ and $\mathbf{p}_i$ are the vector position and linear momentum of i, respectively, and μ is the reduced mass of the binary system. Therefore, relation 13 selects a subset of particles within the multidimensional configurational and momentum space. Unlike the original work by Hill, which dealt with pairwise additive interactions and resulted in a definition based on pairwise connectivity, our study considers many-body interactions and the cluster definition must be modified accordingly.

Here we consider a configuration of N particles to form a cluster when the interaction energy of any subset of the N particles with the remainder of the system satisfies the condition given by eq 13. When the cluster analysis is performed during MC simulations, all particles are assigned random momentum vectors, $\mathbf{p}_i$, from the Gaussian distribution consistent with the external temperature, and then the condition 13 is evaluated.

We have also used an alternative simplified criterion (B) based only on configurational energies. It is equivalent to A with the assumption that all particles and their groups have the average translational kinetic energy of 3/2 k_BT. Accordingly, eq 13 reduces to

$$u_{ij}(\mathbf{r}_i,\mathbf{r}_j) \le -3/2k_BT \tag{14}$$

Because this simplified criterion selects a subset of the configurational space but considers the full momentum space, the kinetic energies of the reactants and products are the same, and consequently eq 4 becomes

$$\Delta H^\circ_{n-1,n}[\mathrm{A}] = U[\mathrm{A}(\mathrm{H_2O})_n] - U[\mathrm{A}(\mathrm{H_2O})_{n-1}] - RT^\circ$$

For cluster ions at 298.15 K, this criterion corresponds roughly to the average ion−water interaction energy at a distance of 10 Å from the central ion, which is the diameter of the cluster-containing cavity used by Lukyanov et al.[51] Results based on our energetic criterion B will therefore correspond closely to those that would be obtained according to this geometric definition.

2.3. Classical Models of Aqueous Electrolytes.

2.3.1. Nonpolarizable Model Based on the SPC/E Water. The simplest force field considered in this study is represented by a rigid nonpolarizable interaction-site model of water and ions, in which the functional form of the site−site potential combines Lennard-Jones (LJ) and point charge interactions, i.e.,

$$U_{IW}(\mathbf{r}_{IW}) = \sum_{j=1}^{N} 4\varepsilon_{IO}\left[\left(\frac{\sigma_{IO}}{|\mathbf{r}_I - \mathbf{r}_{jO}|}\right)^{12} - \left(\frac{\sigma_{IO}}{|\mathbf{r}_I - \mathbf{r}_{jO}|}\right)^{6}\right] + \sum_{j=1}^{N}\sum_{s=1}^{S}\frac{q_I q_s}{|\mathbf{r}_I - \mathbf{r}_{js}|} \tag{15}$$

Here $U_{IW}(\mathbf{r}_{IW})$ is the energy of interaction between ion I and surrounding N water molecules; ε_{IO} and σ_{IO} are the Lennard-Jones energy and size parameters of the ion−water oxygen, IO, interaction; q_I and q_s are charges on ion I and site s of a water molecule, respectively; and expression $|\mathbf{r}_I - \mathbf{r}_{js}|$ denotes the distance between ion I and site s on water molecule j. The model was developed by Joung and Cheatham[23] for use with the SPC/E water[56] with the ion−water force field parameters optimized against multiple experimental properties including ion radii, hydration free energies at infinite dilution, crystal geometry, and lattice energy, as well as *ab initio*-derived energies of selected cluster configurations. The resulting parameters are summarized in Table S1 (Supporting Information). This force field has been used earlier to study the adequacy of the cluster-pair based approximation, which required only relative cation−anion thermodynamics.[19] In contrast, here we use them to calculate the absolute values of the corresponding quantities.

2.3.2. Polarizable Model Based on the SWM4-DP Water. The SWM4-DP model shares the Lennard-Jones and point charge functional form with the SPC/E-based model, eq 15, but adds polarizable interaction on the oxygen site through the Drude charge-on-spring scheme.[57] The interactions between an ion and N water molecules are defined by the following expression:

$$U_{IW}(\mathbf{r}_{IW}) = \sum_{j=1}^{N} 4\varepsilon_{IO}\left[\left(\frac{\sigma_{IO}}{|\mathbf{r}_I - \mathbf{r}_{jO}|}\right)^{12} - \left(\frac{\sigma_{IO}}{|\mathbf{r}_I - \mathbf{r}_{jO}|}\right)^{6}\right] + \sum_{j=1}^{N}\sum_{s=1}^{S}\left[\frac{(q_I - \delta q)q_s}{|\mathbf{r}_I - \mathbf{r}_{js}|} + \frac{\delta q q_s}{|\mathbf{r}_D - \mathbf{r}_{js}|}\right] + \frac{1}{2}k_D|\mathbf{r}_I - \mathbf{r}_D|^2 \tag{16}$$

Here δq is the charge of the Drude particle D, $\mathbf{r}_D$ is its position vector, and k_D is the force constant of the harmonic potential between the ion I and the particle D, where the remaining symbols have the same meaning as in eq 15. The model was optimized using scaled *ab initio*-based polarizabilities, binding energies of ion−water dimers at 298.15 K, and bulk hydration free energies of neutral ion pairs.[24] The resulting parameters are summarized in Table S1 (Supporting Information).

2.3.3. Polarizable Model Based on the BK3 Water. The BK3 model uses Gaussian charges to represent the Coulombic interactions and the Buckingham (exponential-6) potential to describe the non-Coulombic interactions. The water molecule polarizability is implemented through three Drude particle-on-spring sites located at the oxygen and two hydrogen atoms so that the ion−water interaction energy can be written as follows,[28,58]

DOI: 10.1021/jp509401d
J. Phys. Chem. A 2015, 119, 488−500

$$U_{IW}(\mathbf{r}_{IW}) = \sum_{j=1}^{N}\left[A_{IO}\exp(-B_{IO}|\mathbf{r}_I - \mathbf{r}_{jO}|) - \frac{C_{IO}}{|\mathbf{r}_I - \mathbf{r}_{jO}|^6}\right] + \sum_{j=1}^{N}\sum_{s=1}^{S}\left[\frac{(q_I - \delta q)q_s}{|\mathbf{r}_I - \mathbf{r}_{js}|}\,\mathrm{erf}(|\mathbf{r}_I - \mathbf{r}_{js}|\gamma_{Ij}) + \frac{\delta q q_s}{|\mathbf{r}_D - \mathbf{r}_{js}|}\,\mathrm{erf}(|\mathbf{r}_D - \mathbf{r}_{js}|\gamma_{Ij})\right] + \frac{1}{2}k_D|\mathbf{r}_I - \mathbf{r}_D|^2 \quad (17)$$

Here A_{IO}, B_{IO}, and C_{IO} are the parameters of the Buckingham potential between the ion I and the water oxygen O; $\gamma_{Is} = (2\sigma_I^2 + 2\sigma_s^2)^{-1/2}$, with σ_I and σ_s being the width of the Gaussian charges on ion I and water site s, respectively; and the remaining symbols have the same meaning as in eq 16. The entire set of BK3 parameters is summarized in Table S1, Supporting Information. The model was optimized to reproduce experimental hydration free energies of neutral alkali metal halide salts in infinitely diluted bulk solutions, hydration free energy differences within the same-charge series of alkali metal and halide ions, the energy and distance of ion−water dimer energy minimum, and crystal density.[59]

2.4. Classical Monte Carlo Simulations. The microstructural properties and enthalpies of ion hydration involving clusters with n = 1−6 water molecules were calculated from the isochoric−isothermal Monte Carlo (*NVT*-MC). The hydration Helmholtz free energies were calculated from a series of GCMC[60] simulations in which the water chemical potential, $\mu_i(T,V)$, was fixed at different values (corresponding to the changing water vapor pressure in the experiment) and the statistics of cluster sizes was analyzed using the histogram reweighting technique[45] as described elsewhere.[19] Additionally, the Helmholtz free energies were also calculated from trial water molecule insertions and deletions performed during the *NVT*-MC runs.

All simulations were performed in a 28 × 28 × 28 Å box at 298.15 K, with the particle interactions truncated at a cutoff distance of 12 Å, which is sufficient to minimize errors from incorrectly excluding clusters on the basis of our definitions A and B (section 2.2). The length of *NVT*-MC simulations exceeded 1×10^8 individual translational and rotational MC steps, and the combined length of the GCMC simulations for each ion was at least 1×10^9 individual translational, rotational, and insertion/deletion MC steps, where the translations and rotations were accomplished with multiparticle moves.[61] Both the MC simulations and histogram reweighting were performed using in-house codes.

Before proceeding, we need to provide the following details on the calculation of $\Delta F(n,n-1)$: In eqs 5−7 we assumed that the cluster occupies the full phase space available to an ion and n water molecules in the volume V. However, to account for the definition of a cluster as occupying only a subset of the full phase space (section 2.2), we have to modify the equations for the probability of a cluster formation to satisfy our definitions A and B. The partition function and the histogram can be separated into cluster and noncluster parts as follows:

$$Q(n) = Q_c(n) + Q_{\bar{c}}(n) = Q_c(n)\left(1 + \frac{Q_{\bar{c}}(n)}{Q_c(n)}\right)$$

$$\mathcal{H}_i(n) = \mathcal{H}_{c,i}(n) + \mathcal{H}_{\bar{c},i}(n) = \mathcal{H}_{c,i}(n)\left(1 + \frac{\mathcal{H}_{\bar{c},i}(n)}{\mathcal{H}_{c,i}(n)}\right) \quad (18)$$

where the subscript c denotes the part of the canonical partition function pertaining to clusters and $\bar{c}$ denotes its complement. Equation 7 can then be rewritten as follows:

$$\beta\{F_c[A(H_2O)_n] - F_c[A(H_2O)_{n-1}]\} = -\ln\left[\frac{\mathcal{H}_{c,i}(n)}{\mathcal{H}_{c,i}(n-1)}\right] + \beta\mu_i = \beta\{F[A(H_2O)_n] - F[A(H_2O)_{n-1}]\} + \ln\left[\frac{1 + \mathcal{X}(n)}{1 + \mathcal{X}(n-1)}\right] \quad (19)$$

where $\mathcal{X}(n) = \mathcal{H}_{\bar{c}}(n)/\mathcal{H}_c(n)$ is the ratio of nonclusters to clusters in a simulation box with n water molecules, which can be obtained from both *NVT*-MC or GCMC simulations.

2.5. Density Functional Theory Simulations. The microstructural properties of small ion−water clusters can be efficiently studied by simulations in which the particle interactions are determined using quantum chemical methods. Although the present simulations do not explicitly take into account purely quantum effects, such as the zero-point energy or proton tunneling, it has been shown that the structural features, including the peak positions of radial distribution functions analyzed in the present study, are rather insensitive to them.[62]

The cluster ions were studied using *NVT*-MC simulations with potential energies determined from the quantum density functional theory (DFT). In particular, a hybrid generalized-gradient approximation (GGA) density functional ω-B97X-D with long-range dispersion corrections[63] was used because it was found to accurately reproduce the results of higher-level *ab initio* methods for water clusters.[64] Dunning's correlation-consistent basis sets of double-ζ quality augmented with diffuse functions were used for that purpose.[65] All calculations were performed using Gaussian 09 program package[66] implemented as a back-end for a nested Monte Carlo simulation program.[67] Computationally inexpensive flexible empirical potentials[68,69] in the inner part were subsequently corrected by accurate but computationally expensive DFT potential energies in the outer part. The magnitude and number of inner Monte Carlo steps were tuned to keep the corresponding acceptance probabilities reasonably high. The initial parts of simulations were discarded and the simulations were run until several thousands of independent samples of cluster configurations were accumulated.

3. RESULTS AND DISCUSSION

3.1. Pure Water Clusters. Before analyzing cluster-ion properties, it is helpful to assess the ability of molecular models to describe water−water interactions in pure water clusters. For that purpose we illustrate in Figure 1 the evolution of the calculated incremental hydration free energies and enthalpies of water at 298.15 K, which are also listed in Table S2 in the Supporting Information document. We note that the experimentally based estimates of properties of water clusters derived from thermodynamic considerations and virial coefficients[18,70−73] cannot be directly compared with the

DOI: 10.1021/jp509401d
J. Phys. Chem. A 2015, 119, 488−500

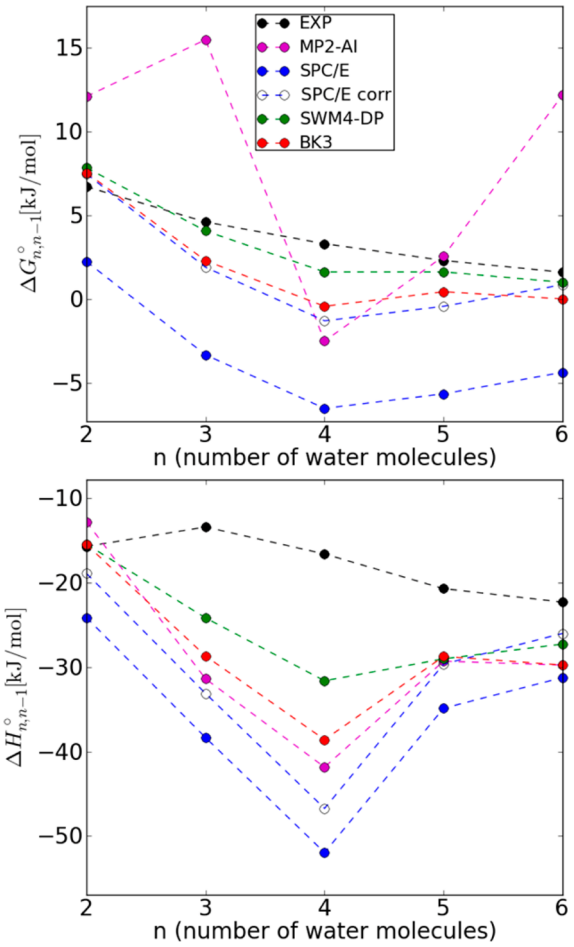

Figure 1. Incremental hydration Gibbs free energies (top) and enthalpies (bottom) of pure water clusters: experiment[70,71] (black), SPC/E (blue, filled circles), polarization corrected SPC/E (blue, open circles), SWM4-DP (green), BK3 (red), and MP2-level *ab initio*[74] (magenta).

clusters on the basis of the present definitions, which, unlike the experimental estimates, assume zero cluster−cluster interactions in water vapor (e.g., see related discussion by Hill[52]). Nevertheless, as a reference, we display the experimental estimates along with our results and also include values from quantum chemical calculations taken from the available literature.[74]

As a first step, we analyzed the effect of the cluster definition (section 2.2) on the calculated thermodynamic properties. The resulting properties according to both cluster definitions (listed in Table S2, Supporting Information) differ from each other by less than 1 kJ/mol, a difference significantly smaller than the absolute values of $\Delta G^{\circ}_{n-1,n}$ and $\Delta H^{\circ}_{n-1,n}$. Consequently, following qualitative discussion can be considered valid for either cluster definition.

The statistical errors of the calculated thermodynamic properties of water clusters differ depending on the simulation methodology. Our classical simulation results were evaluated using the block method and the standard deviation was estimated to be less than 0.2 kJ/mol. The statistical errors of quantum mechanical results are not discussed in detail in the original literature, but the authors suggest deviations in the order of units of kJ/mol.[74] In addition systematic errors inherent in various quantum chemical methods have to be considered.

In Figure 1 we plot the incremental hydration Gibbs free energies and enthalpies of water clusters from the three water models against *ab initio* results. Here we can highlight several features. The $\Delta G^{\circ}_{n-1,n}$ and $\Delta H^{\circ}_{n-1,n}$ values predicted by the nonpolarizable SPC/E model are consistently more negative than those predicted by the polarizable models. However, note that this direct comparison does not take into account the self-polarization correction of ∼5.23 kJ/mol built into the model, which represents the intramolecular energy needed to increase the water dipole moment from its vacuum value (1.85 D) to that of the SPC/E model (2.35 D).[56] Because the SWM4-DP and BK3 models include this contribution in the total thermodynamic properties, it should also be added to the SPC/E results to make consistent comparisons. After adding the correction, the SPC/E results are in close agreement with the polarizable models; in fact, the agreement between the corrected SPC/E and BK3 predictions of $\Delta G^{\circ}_{n-1,n}$ is better than that between the two polarizable models. It is somewhat surprising that a model as simple as the SPC/E can describe gas phase−water interactions so close to much more complex force fields. This observation may indicate that short-range hydrogen bond interactions (as opposed to longer-range dipolar interactions) are the dominant contributor to cluster thermodynamics and have similar strength in the gas and liquid phases. The agreement between *ab initio* calculations and SPC/E simulated $\Delta G^{\circ}_{n-1,n}$ along with a more negative deviation for $\Delta H^{\circ}_{n-1,n}$ suggests more localized hydrogen bonds resulting in structures characterized by low energy and low entropy (Table S2, Supporting Information). However, despite the favorable predictions of the SPC/E model, we cannot generalize these observations to other empirical force fields, whose cluster property predictions can differ qualitatively.[75]

Another notable trend present in Figure 1 is the significant difference between the quantum chemical and classical model predictions showing up for the $\Delta G^{\circ}_{n-1,n}$, which is surprising given the close agreement of $\Delta H^{\circ}_{n-1,n}$. The reason for the discrepancy may lie in significant statistical errors, but potentially also in the "Boltzmann averaging over low energy structures", as described in the original literature.[74] Such averaging could lead to underestimation of higher energy configurations, which contribute more significantly to the system's entropy.

A distinctive feature of all classical simulation results in Figure 1 is the presence of a minimum in the size dependence of the cluster properties corresponding to tetramer clusters. Further analysis of the results and comparison with quantum chemical studies in the literature[74] suggests that mechanism underlying this minimum is the formation of remarkably stable cyclical configurations. These configurations can be also identified through the presence of the next-nearest neighbor peak at 4 Å in the plot of oxygen−oxygen pair distribution functions for n = 4, as illustrated in Figure 2. The minimum appears more pronounced for $\Delta H^{\circ}_{n-1,n}$ than for $\Delta G^{\circ}_{n-1,n}$, indicating an underlying trade-off between energetic favorability of the ring structures and their unfavorably low entropy. Incorporation of an additional water molecule (n = 5) to the cluster will result in a more loosely bound structure, as evidenced by the lower incremental enthalpy and the wide second peak in Figure 2.

3.2. Ion−Water Clusters. To evaluate the uncertainty associated with the cluster definition, we calculated the cluster-

DOI: 10.1021/jp509401d
J. Phys. Chem. A 2015, 119, 488−500

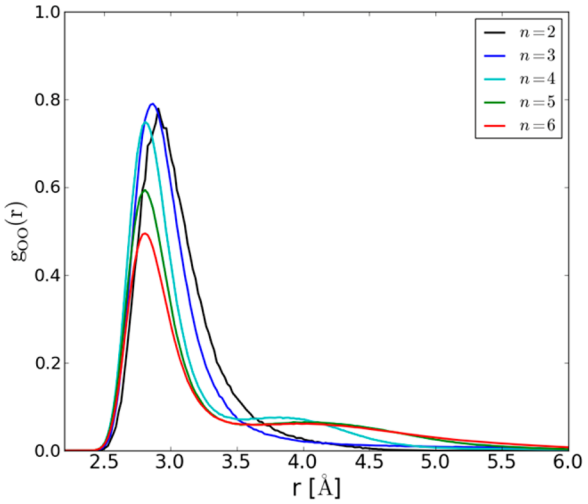

Figure 2. Oxygen−oxygen pair distribution functions for BK3 water clusters, n = 2−6.

ion thermodynamics on the basis of our two criteria, A and B (section 2.2). The resulting two sets of $\Delta G^{\circ}_{n-1,n}$ and $\Delta H^{\circ}_{n-1,n}$ listed in Tables S4−S6 (Supporting Information) differ by less than 0.01 kJ/mol, which is less than the statistical uncertainty associated with the simulated quantities. Therefore, for all practical purposes, the following discussion can be considered valid for either cluster definition. Only a small fraction (0−2%) of the generated configurations was classified as nonclusters, which highlights the large stability of the systems where all water molecules are contained within the deep Coulombic potential well of the central ion and form its first hydration shell. The observed stability also reduces the uncertainty about the proper cluster definition.

As in the case of pure water clusters, the statistical error in terms of the standard deviation of our classical simulations was less than 0.2 kJ/mol; therefore, the error bars would be smaller than the symbol sizes in the data plots. The standard deviation of Na^+ hydration enthalpies derived from our quantum chemical simulations ranged from 0.11 to 2.31 kJ/mol for clusters of n = 1 and n = 5, respectively. The experimental errors differ for each methodology. For anions the reported

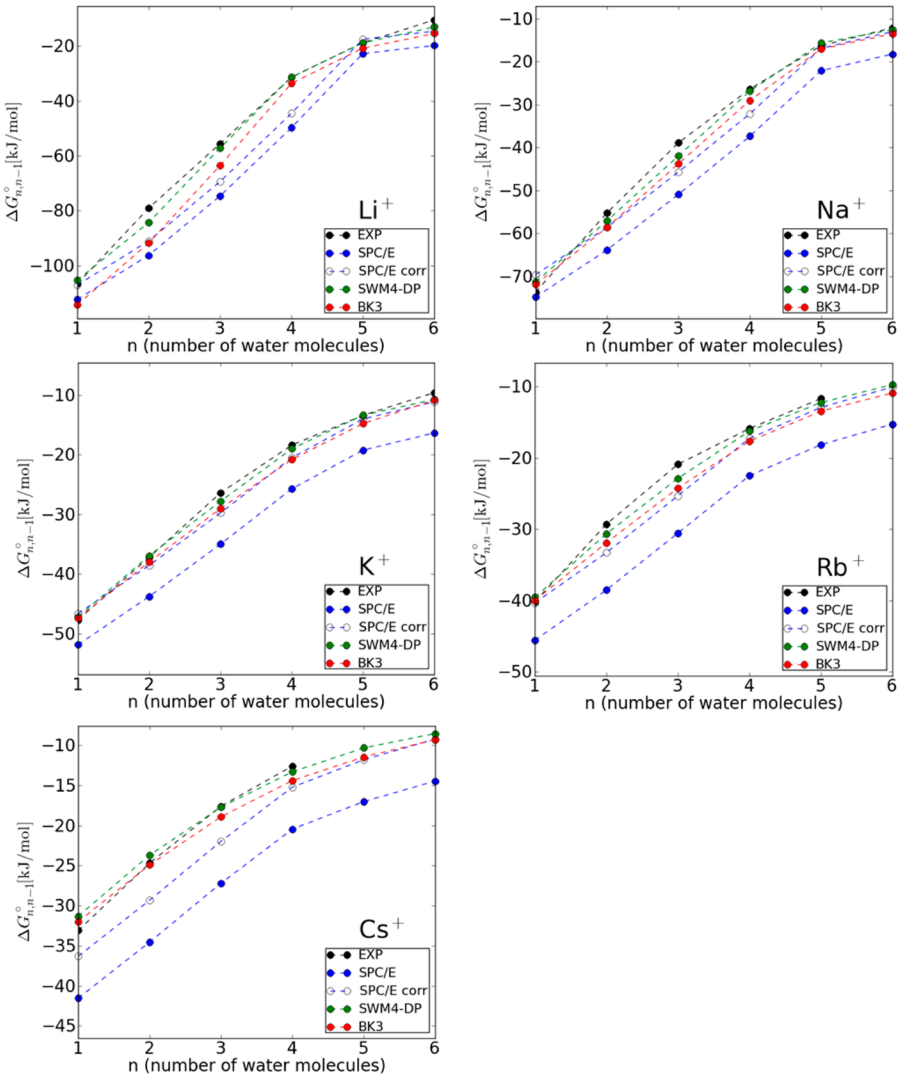

Figure 3. Incremental hydration Gibbs free energies of alkali metal ions: HPMS experiment[13] (black), SPC/E (blue, filled circles), polarization corrected SPC/E (blue, open circles), SWM4-DP (green), and BK3 (red).

DOI: 10.1021/jp509401d
J. Phys. Chem. A 2015, 119, 488−500

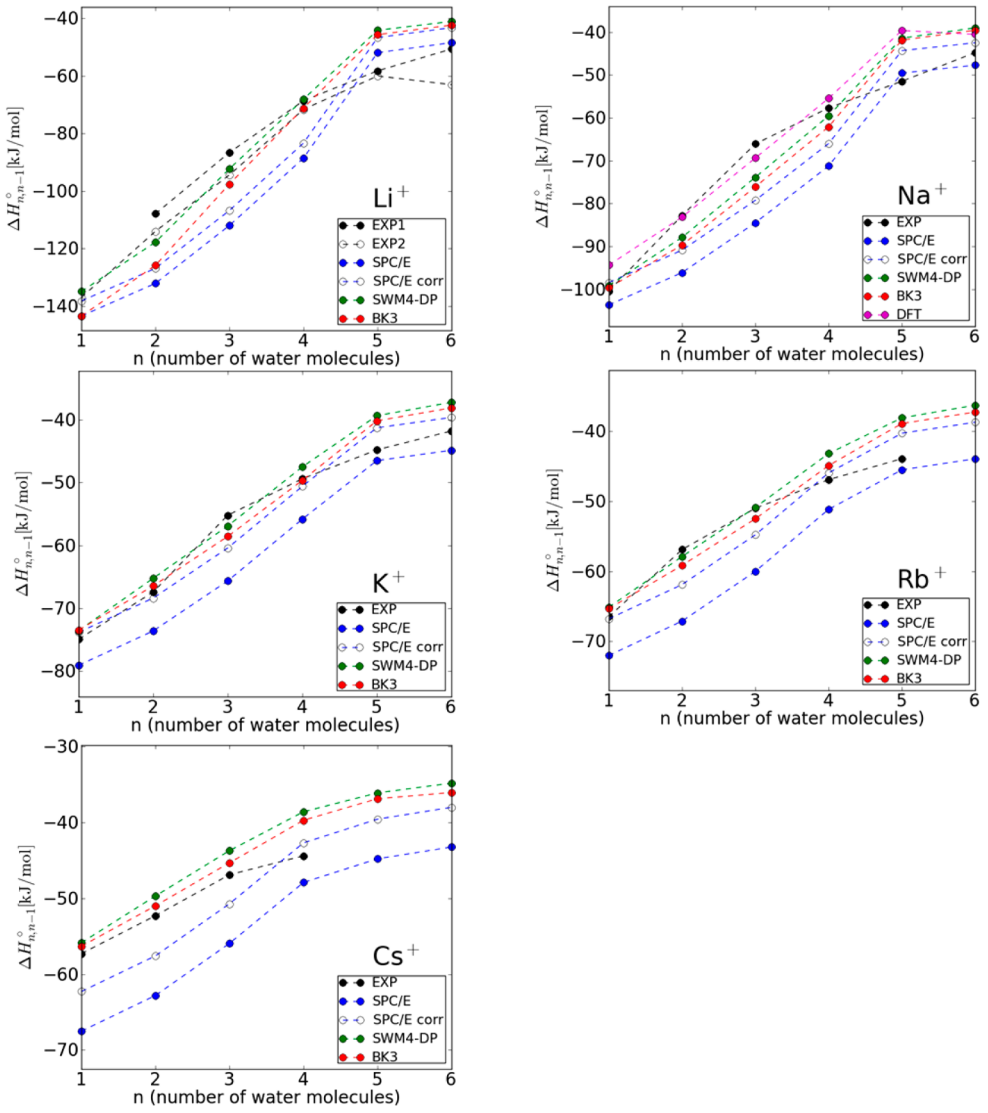

Figure 4. Incremental hydration enthalpies of alkali metal ions: HPMS experiment[13] (black, filled circles), CID experiment[16,17] (black, open circles), SPC/E (blue, filled circles), polarization corrected SPC/E (blue, open circles), SWM4-DP (green), BK3 (red), and DFT (magenta).

standard deviations are around 5 kJ/mol or lower[14] but can reach 10 kJ/mol or more for cations.[76]

The hydration structure and thermodynamics of cations and anions differ qualitatively as a result of water molecule asymmetry, and these differences persist over clusters of all sizes.[19] The main contribution to ion hydration energies in the small clusters investigated here comes from contact interactions in the first hydration shell. For cations, the dominant attractive term is the Coulombic interaction with water oxygens, whereas for anions, it comes from strong hydrogen bonding that involves purely quantum mechanical effects,[77] and whose proper description is often difficult even with more sophisticated classical force fields.

The plots of cationic $\Delta G^{\circ}_{n-1,n}$ in Figure 3 show that the overall agreement of the two polarizable models with the high pressure mass spectrometry (HPMS) experimental data of Dzidic and Kebarle[13] is nearly quantitative for most ions, whereas the nonpolarizable model predictions are consistently shifted to more negative values. As in the case of pure water clusters, most of the shift can be explained by the SPC/E self-polarization correction. In the case of larger cations (i.e., K^+ and Rb^+), the corrected SPC/E values are in close agreement with the predictions of the polarizable models over the full range of cluster sizes. Even in the case of the smallest Li^+ ion, for which the largest induced water dipoles are detected, the corrected nonpolarizable predictions do not significantly deviate from the behavior of more complex force fields. The large constant deviation of the Cs^+ values seems to be caused by the particular choice of the LJ parameters rather than a failure of the nonpolarizable representation. Indeed, the LJ parameters of the Cs^+-H_2O interaction deviate strongly from the trend established by smaller cations (Table S1, Supporting Information), which may indicate difficulties in their optimization that aimed to reproduce not only aqueous solution properties but also those of alkali metal halide crystals.[23]

The trends seen for cationic $\Delta G^{\circ}_{n-1,n}$ are reproduced and magnified in the plots of $\Delta H^{\circ}_{n-1,n}$ in Figure 4. There is very little difference between the predictions of the two polarizable models despite their contrasting functional descriptions of the Coulombic and non-Coulombic interactions, including the polarization sites. The corrected SPC/E model values are also in close agreement with the polarizable models, suggesting that the effective treatment of water molecule polarization may be

DOI: 10.1021/jp509401d
J. Phys. Chem. A 2015, 119, 488−500

considered reasonably justified even for the cluster cation systems. However, even though the model predictions are mutually similar, they all fail to reproduce the trends seen in the experimental results. In particular, the simulated dependence of $\Delta H^{\circ}_{n-1,n}$ for n = 1−5 is convex (bends upward), whereas the experimentally determined dependence is concave, which leads to large deviations for midsize clusters. For instance, $\Delta H^{\circ}_{2,3}[Na^+]$ differs by as much as ∼10 kJ/mol for the most accurate model included in the comparison. Moreover, the simulation results exhibit a sharp change in their trend at n = 5, a behavior not observed in experiments.

It is not immediately clear why the above models deviate from the experimental results. In fact, similar discrepancies between the experiment and a simple electrostatic model were noted and discussed in the original paper by Dzidic and Kebarle,[13] who suggested that some form of covalency may be missing from the interaction model. To test this hypothesis, we have plotted in Figure 4 a comparison between the model descriptions and our quantum chemical simulation results for the hydration enthalpies, from which we can observe an obvious resemblance between the quantum and classical data. Moreover, our preliminary simulations with the popular AMOEBA force field yielded a similar convex dependence for $\Delta H^{\circ}_{n-1,n}[Li^+]$ and $\Delta H^{\circ}_{n-1,n}[Na^+]$ in close agreement with the quantum chemical results. These results raise the question of plausible explanations behind the observed discrepancies. The differences may be the result of neglected or underrepresented ion−water interactions, such as charge transfer effects,[78] in the computational models. Alternatively, they may result from inaccurate assumptions built into the experimental method, which involves extrapolations from high temperature measurements to 298.15 K, or simply the experimental statistical error. Even though the trends of cation hydration enthalpies from the HPMS experiments appear smooth without statistical noise,[13] the overall errors estimated from other methods reach up to ∼10 kJ/mol,[76] which could explain the differences. In support of the contention that HPMS experimental data, rather than the models, may be the culprit of the discrepancy, an alternative set of data for the enthalpies of Na^+ hydration (n = 1−4) at 0 K based on the collision-induced dissociation experiments appear more consistent with the classical and quantum simulation results than those from the HPMS experiments.[16]

The analysis of the cluster structural properties can facilitate the microscopic interpretation of the observed hydration thermodynamics, as illustrated in Figure 5 where we compare the ion−oxygen pair distribution functions for Li^+ and Na^+ clusters with n = 1 and 5, as predicted by the classical models, and DFT calculations. The main distinctive feature in this comparison is the shift to shorter separations of the first peak of the BK3 distribution functions. Interestingly, our DFT data are most closely matched by the SPC/E model.

The incremental hydration Gibbs free energies of halide anion hydration presented in Figure 6 indicate that the overall agreement of the modeling with experimental data is poorer than for alkaline cations. The largest discrepancies are seen for the SPC/E-based model of small F^- clusters even if the polarization correction is included. The SWM4-DP model predictions also deviate significantly for the lowest values of n, but gradually improve for heavier halide ions. The BK3 model predictions are nearly in quantitative agreement for the F^- systems, but the model's performance deteriorates with the increasing atomic weight of the halide ion. A likely explanation for the satisfactory description of the F^- clusters by the BK3

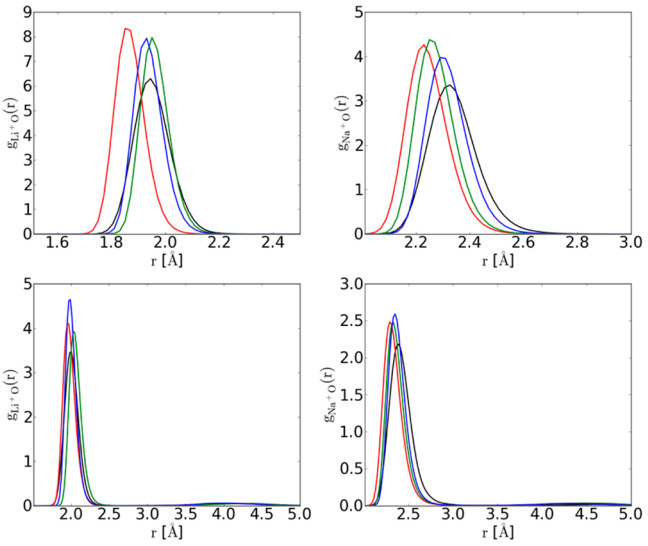

Figure 5. Ion−oxygen pair distribution functions for Li^+ (left) Na^+ (right) cluster ions with n = 1 (top) and n = 5 (bottom) predicted by SPC/E (blue), SWM4-DP (green), and BK3 (red) models and DFT potential (black).

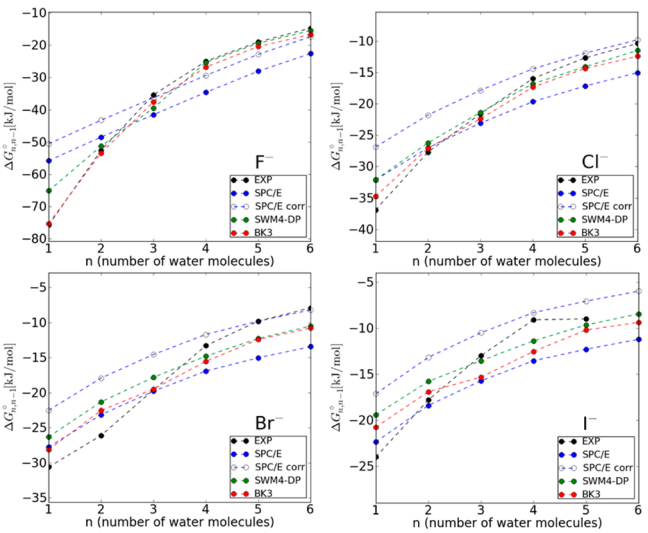

Figure 6. Incremental hydration Gibbs free energies of halide ions: HPMS experiment[14] (black), SPC/E (blue, filled circles), polarization corrected SPC/E (blue, open circles), SWM4-DP (green), and BK3 (red).

model lies in its use of three polarizable sites, two of which are located at the hydrogens. As discussed in the early work by Arshadi and co-workers,[79] the large negative energy of the first stepwise hydration reaction, $F^- + H_2O \rightarrow F^-(H_2O)$ may be caused by the partial charge and proton transfer in the strong hydrogen bond $F^-\cdots H^+\cdots OH^-$ (see Figure 7). Although the current rigid nonreactive models cannot accurately reproduce such interactions, the charge-on-spring hydrogen of the BK3 model can emulate their effects. This is not possible for the SPC/E and SWM4-DP representations; consequently, they fail to reproduce the hydration trends not only for the F^- clusters but also for the remaining halides. A systematic investigation of the SPC/E-based alkali metal halide models confirms that the observed discrepancies between model predictions and HPMS do not come from the model's parametrization but from its

DOI: 10.1021/jp509401d
J. Phys. Chem. A 2015, 119, 488−500

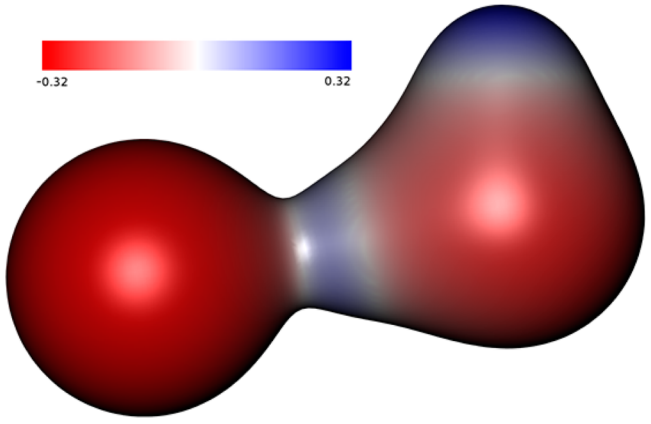

Figure 7. Electrostatic potential around an F^-–H_2O dimer in atomic units (au) at the contour of electronic density of 0.05 au.

functional form, and that the unsatisfactory reproduction of anion–water interactions extends to bulk solution properties.[19]

To further test our conjecture about the origin of the qualitative trends, i.e., functional form versus parametrization, we calculated cluster ion hydration thermodynamics using a nonpolarizable force field developed by Dang and others[80,81] and later used in combination with the SPC model of water[82] by Rajamani et al.[83] The comparison of these results with experiment and our original SPC/E-based set developed by Joung and Cheatham[23] is included in the Supporting Information in Table S7 and Figures S1–4. It can be seen that, although the absolute values of the predicted free energies and enthalpies are vertically shifted (the SPC-based results typically lie between the corrected and uncorrected SPC/E-based predictions), the trend lines are nearly parallel. This is especially true for anions, where the slopes of n-dependence for different halide ions are essentially identical; this is despite the fact that not only ion–water LJ parameters are changed but also the water model charge distribution is altered. These findings further support the idea that a qualitative change of stepwise hydration trends requires qualitative changes in the model construction.

The behavior of $\Delta H^\circ_{n-1,n}$ for halide anions illustrated in Figure 8 demonstrates that a reasonable prediction of hydration free energies does not guarantee correct enthalpies (or entropies for that matter). Although the discrepancies in the SPC/E and SWM4-DP model predictions are qualitatively the same as in the case of $\Delta G^\circ_{n-1,n}$, an unexpected behavior is exhibited by the BK3 model for $\Delta H^\circ_{2,3}[X^-]$, where X = Cl, Br, or I. Unlike the experiment or other models, including the AMOEBA force field,[33] the BK3 model predicts a sharply lower enthalpy when the third water molecule is added to the cluster. A closer look at the generated low energy structures reveals the formation of a symmetric pyramidal structure as depicted in Figure 9. The relative stability of this configuration was observed in quantum chemical calculations for all halide ions,[84,85] but it is clearly exaggerated by the BK3 model. This artifact illustrates the challenges underlying the development of accurate molecular models and the need for their thorough testing.

Finally, in Figure 10 we compare the ion–oxygen and ion–hydrogen pair distribution functions for selected F^- clusters predicted by classical and *ab initio* simulations, where we observe, as in the case of Li^+ and Na^+ ions (Figure 5), that the peaks of the BK3 model distribution functions are shifted to

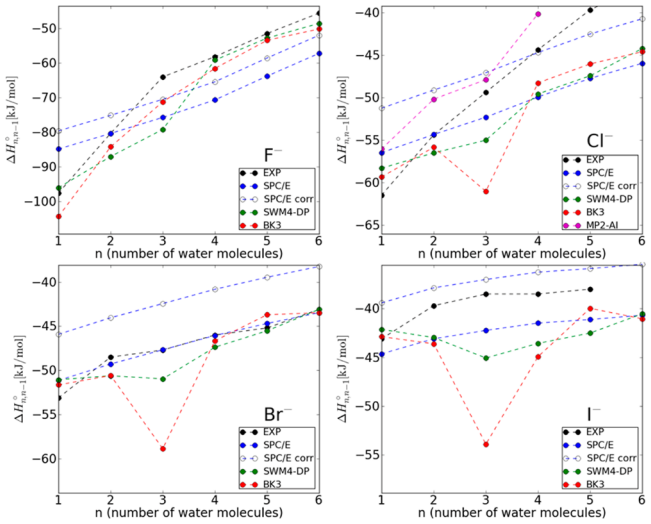

Figure 8. Incremental hydration enthalpies of halide ions: HPMS experiment[14] (black, filled circles), SPC/E (blue, filled circles), polarization corrected SPC/E (blue, open circles), SWM4-DP (green), BK3 (red), and MP2-level *ab initio*[85] (magenta).

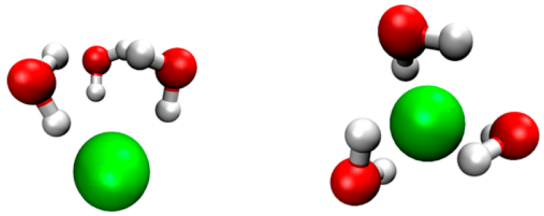

Figure 9. Side (left) and top (right) view of the stable pyramidal structure formed by BK3 $Cl^-(H_2O)_3$ clusters.

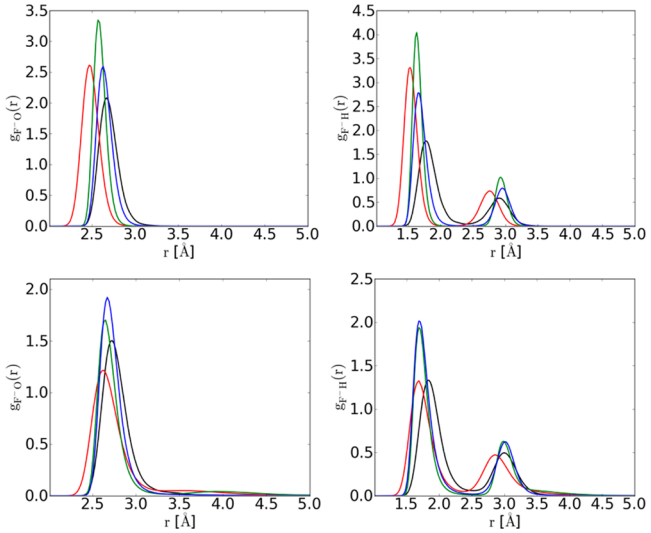

Figure 10. Ion–oxygen (left) and ion–hydrogen (right) pair distribution functions for F^- clusters with n = 1 (top) and n = 5 (bottom) predicted by the SPC/E (blue), SWM4-DP (green), and BK3 (red) models and DFT potential (black).

shorter separations compared to both the SPC/E and quantum results. The shorter H_2O–F^- distances may be required to compensate for the decreased ion–hydrogen attraction resulting from the overlapping Gaussian charges.

DOI: 10.1021/jp509401d
J. Phys. Chem. A 2015, 119, 488–500

4. CONCLUSIONS

We have tested the ability of classical molecular models to describe the microstructural and thermodynamic behavior of gas-phase hydration of alkali metal and halide ions, as well as the formation of small water clusters. In particular, we investigated the effect of many-body interactions (polarization) and charge penetration on determining the incremental hydration Gibbs free energy and corresponding enthalpy. For that purpose we employed three contrasting models including (i) point charge nonpolarizable SPC/E, (ii) Drude point charge polarizable SWM4-DP, and (iii) Drude Gaussian charge polarizable BK3.

We have performed a series of classical and quantum chemical simulations of gas-phase ion hydration at 298.15 K to assess the performance of force field parametrizations of the above models. Even though it is not always possible to distinguish between the failings of a specific parametrization from the deficiencies of the interaction model itself, the resulting extensive data sets and the analysis of hydration trends allowed us to draw more general conclusions about the factors controlling the ion hydration process while simultaneously raising questions about the accuracy of the available experimental data.

In general, the investigated classical models are able to describe alkali metal cationic clusters more accurately than the halide anionic counterparts. Even though there is a significant disagreement between the experimental Na^+ hydration enthalpies of Dzidic and Kebarle[13] and the corresponding modeling results based on quantum chemical or classical simulations, it appears that even very simple nonpolarizable models using point charges and Lennard-Jones interactions can capture the essence of the cation−water interactions. Water−anion interactions involving the formation of strong hydrogen bonds appear as a more complex hydration process, which requires incorporation of many-body effects. Our analysis of the SWM4-DP and BK3 polarizable models suggests that a single polarizable site located at, or near, the oxygen center may not be sufficient to reproduce the hydration thermodynamic trends seen in experimental data, which was only achievable through additional polarizable sites located at the hydrogen atoms, as in the case of BK3 and AMOEBA force fields. As we might have expected, the overall agreement between model predictions and experimental data improves with increasing model complexity. However, even adequate description of the hydration thermodynamics does not guarantee overall agreement of the cluster ion structural properties, as highlighted by the example of the BK3 model description of $Cl^-(H_2O)_3$ clusters.

The combination of classical and quantum chemical simulations, together with the alternative CID experiments, indicates that there might be underlying inaccuracies in the high-pressure mass spectrometry determination of small cation hydration. Although the present study cannot conclusively answer this question, or pinpoint their sources, it highlights issues that will have to be resolved in order to develop and validate predictively accurate models of ion−water interactions.

■ ASSOCIATED CONTENT

Supporting Information

Tabulated simulation results (force field parameters, Gibbs free energies, enthalpies, dipole moments) and complementary plots (Gibbs free energies, enthalpies). This material is available free of charge via the Internet at http://pubs.acs.org.

■ AUTHOR INFORMATION

Corresponding Author

*L. Vlcek. E-mail address: vlcekl1@ornl.gov.

Notes

The authors declare no competing financial interest.

■ ACKNOWLEDGMENTS

This research was supported by the U.S. Department of Energy, Office of Science, Basic Energy Sciences, Chemical Sciences, Geosciences, and Biosciences Division. The participation of F.M. and I.N. was facilitated by the Czech-USA cooperative research program "Nonadditive interactions in aqueous solutions of electrolytes". F.U. thanks the Czech Science Foundation (P208/10/1724) and is thankful for access to the CERIT-SC computing facilities (CZ.1.05/3.2.00/08.0144)

■ REFERENCES

(1) Ferguson, E. E. Mass Spectrometry in Ionospheric Research. *Mass Spectrom. Rev.* **2007**, *26*, 142−149.

(2) Ghosal, S.; Hemminger, J. C.; Bluhm, H.; Mun, B. S.; Hebenstreit, E. L. D.; Ketteler, G.; Ogletree, D. F.; Requejo, F. G.; Salmeron, M. Electron Spectroscopy of Aqueous Solution Interfaces Reveals Surface Enhancement of Halides. *Science* **2005**, *307*, 563−566.

(3) Hayhurst, A. N.; Sugden, T. M. Mass Spectrometry of Flames. *Proc. R. Soc. A* **1966**, *293*, 36−50.

(4) Hayhurst, A. N. Mass Spectrometric Sampling of a Flame. *Combust. Explos. Shock Waves* **2012**, *48*, 516−525.

(5) Hvelplund, P.; Pedersen, J. O. P.; Stochkel, K.; Enghoff, M. B.; Kurten, T. Experimental Studies of the Formation of Cluster Ions Formed by Corona Discharge in an Atmosphere Containing SO_2, NH_3, and H_2O. *Int. J. Mass. Spectrom* **2013**, *341*, 1−6.

(6) Pitzer, K. S.; Palaban, R. T. Thermodynamics of NaCl in Steam. *Geochim. Cosmochim. Acta* **1986**, *50*, 1445−1454.

(7) Chialvo, A. A.; Gruszkiewicz, M. S.; Cole, D. R. Ion-Pair Association in Ultrasupercritical Aqueous Environments: Successful Interplay among Conductance Experiments, Theory, and Molecular Simulations. *J. Chem. Eng. Data* **2010**, *55*, 1828−1836.

(8) Kebarle, P.; Verkerk, U. H. Electrospray: From Ions in Solution to Ions in the Gas Phase, What We Know Now. *Mass Spectrom. Rev.* **2009**, *28*, 898−917.

(9) Payzant, J. D.; Yamdagni, R.; Kebarle, P. Hydration of CN^-, NO_2^-, NO_3^-, and OH^- in Gas Phase. *Can. J. Chem.* **1971**, *49*, 3308−3314.

(10) Blades, A. T.; Kebarle, P. Sequential Hydration Energies of the Sulfate Ion, from Determinations of the Equilibrium Constants for the Gas-Phase Reactions: $SO_4(H_2O)_n^{2-} = SO_4(H_2O)_{n-1}^{2-} + H_2O$. *J. Phys. Chem. A* **2005**, *109*, 8293−8298.

(11) Blades, A. T.; Jayaweera, P.; Ikonomou, M. G.; Kebarle, P. Ion−Molecule Clusters Involving Doubly Charged Metal-Ions (M^{2+}). *Int. J. Mass. Spectrom. Ion Processes* **1990**, *102*, 251−267.

(12) Blades, A. T.; Peschke, M.; Verkerk, U. H.; Kebarle, P. Hydration Energies in the Gas Phase of Select $(MX)_mM^+$ Ions, Where $M^+ = Na^+, K^+, Rb^+, Cs^+, NH_4^+$ and X- = F^-, Cl^-, Br^-, I^-, NO_2^-, NO_3^-. Observed Magic Numbers of $(MX)_mM^+$ Ions and Their Possible Significance. *J. Am. Chem. Soc.* **2004**, *126*, 11995−12003.

(13) Dzidic, I.; Kebarle, P. Hydration of Alkali Ions in Gas Phase - Enthalpies and Entropies of Reactions $M^+(H_2O)_{n-1}+H_2O = M^+(H_2O)_n$. *J. Phys. Chem.* **1970**, *74*, 1466−1474.

(14) Hiraoka, K.; Mizuse, S.; Yamabe, S. Solvation of Halide-Ions with H_2O and CH_3CN in the Gas-Phase. *J. Phys. Chem.* **1988**, *92*, 3943−3952.

(15) Amicangelo, J. C.; Armentrout, P. B. Ligand Exchange Reactions of Sodium Cation Complexes Examined Using Guided Ion Beam Mass Spectrometry: Relative and Absolute Dissociation Free Energies and Entropies. *J. Phys. Chem. A* **2004**, *108*, 10698−10713.

DOI: 10.1021/jp509401d
J. Phys. Chem. A 2015, 119, 488−500

(16) Dalleska, N. F.; Tjelta, B. L.; Armentrout, P. B. Sequential Bond-Energies of Water to Na^+ (3s(0)), Mg^+ (3s(1)), and Al^+ (3s(2)). *J. Phys. Chem.* **1994**, *98*, 4191−4195.
(17) Rodgers, M. T.; Armentrout, P. B. Collision-Induced Dissociation Measurements on $Li^+(H_2O)_n$, n=1−6: The First Direct Measurement of the Li^+-OH_2 Bond Energy. *J. Phys. Chem. A* **1997**, *101*, 1238−1249.
(18) Tissandier, M. D.; Cowen, K. A.; Feng, W. Y.; Gundlach, E.; Cohen, M. H.; Earhart, A. D.; Coe, J. V.; Tuttle, T. R. The Proton's Absolute Aqueous Enthalpy and Gibbs Free Energy of Solvation from Cluster-Ion Solvation Data. *J. Phys. Chem. A* **1998**, *102*, 7787−7794.
(19) Vlcek, L.; Chialvo, A. A.; Simonson, J. M. Correspondence between Cluster-Ion and Bulk Solution Thermodynamic Properties: On the Validity of the Cluster-Pair-Based Approximation. *J. Phys. Chem. A* **2013**, *117*, 11328−11338.
(20) Lukyanov, S. I.; Zidi, Z. S.; Shevkunov, S. V. Ion-Water Cluster Free Energy Computer Simulation Using Some of Most Popular Ion-Water and Water-Water Pair Interaction Models. *Chem. Phys.* **2007**, *332*, 188−202.
(21) Shevkunov, S. V. Polarization Effects in $Cl^-(H_2O)_n$ Clusters. Computer Simulation. *Colloid J.* **2009**, *71*, 406−421.
(22) Ren, P. Y.; Ponder, J. W. Polarizable Atomic Multipole Water Model for Molecular Mechanics Simulation. *J. Phys. Chem. B* **2003**, *107*, 5933−5947.
(23) Joung, I. S.; Cheatham, T. E. Determination of Alkali and Halide Monovalent Ion Parameters for Use in Explicitly Solvated Biomolecular Simulations. *J. Phys. Chem. B* **2008**, *112*, 9020−9041.
(24) Lamoureux, G.; Roux, B. Absolute Hydration Free Energy Scale for Alkali and Halide Ions Established from Simulations with a Polarizable Force Field. *J. Phys. Chem. B* **2006**, *110*, 3308−3322.
(25) Dang, L. X. Characterization of Water Octamer, Nanomer, Decamer, and Iodide-Water Interactions Using Molecular Dynamics Techniques. *J. Chem. Phys.* **1999**, *110*, 1526−1532.
(26) Bako, I.; Hutter, J.; Palinkas, G. Car-Parrinello Molecular Dynamics Simulation of the Hydrated Calcium Ion. *J. Chem. Phys.* **2002**, *117*, 9838−9843.
(27) McGrath, M. J.; Kuo, I. F. W.; Ngouana W, B. F.; Ghogomu, J. N.; Mundy, C. J.; Marenich, A. V.; Cramer, C. J.; Truhlar, D. G.; Siepmann, J. I. Calculation of the Gibbs Free Energy of Solvation and Dissociation of Hcl in Water Via Monte Carlo Simulations and Continuum Solvation Models. *Phys. Chem. Chem. Phys.* **2013**, *15*, 13578−13585.
(28) Baranyai, A.; Kiss, P. T. A Transferable Classical Potential for the Water Molecule. *J. Chem. Phys.* **2010**, *133*, 144109.
(29) Fanourgakis, G. S.; Xantheas, S. S. The Flexible, Polarizable, Thole-Type Interaction Potential for Water (TTM2-F) Revisited. *J. Phys. Chem. A* **2006**, *110*, 4100−4106.
(30) Paricaud, P.; Predota, M.; Chialvo, A. A.; Cummings, P. T. From Dimer to Condensed Phases at Extreme Conditions: Accurate Predictions of the Properties of Water by a Gaussian Charge Polarizable Model. *J. Chem. Phys.* **2005**, *122*, 244511.
(31) Yu, H. B.; van Gunsteren, W. F. Charge-on-Spring Polarizable Water Models Revisited: From Water Clusters to Liquid Water to Ice. *J. Chem. Phys.* **2004**, *121*, 9549−9564.
(32) Dang, L. X.; Chang, T. M. Molecular Dynamics Study of Water Clusters, Liquid, and Liquid-Vapor Interface of Water with Many-Body Potentials. *J. Chem. Phys.* **1997**, *106*, 8149−8159.
(33) Grossfield, A.; Ren, P. Y.; Ponder, J. W. Ion Solvation Thermodynamics from Simulation with a Polarizable Force Field. *J. Am. Chem. Soc.* **2003**, *125*, 15671−15682.
(34) Dang, L. X.; Rice, J. E.; Caldwell, J.; Kollman, P. A. Ion Solvation in Polarizable Water - Molecular-Dynamics Simulations. *J. Am. Chem. Soc.* **1991**, *113*, 2481−2486.
(35) Smith, D. E.; Dang, L. X. Computer-Simulations of Cesium Water Clusters - Do Ion Water Clusters Form Gas-Phase Clathrates. *J. Chem. Phys.* **1994**, *101*, 7873−7881.
(36) Smith, D. E.; Dang, L. X. Computer-Simulations of Nacl Association in Polarizable Water. *J. Chem. Phys.* **1994**, *100*, 3757−3766.
(37) Shevkunov, S. V. Charge Separation in $Na^+Cl^-(H_2O)_n$ Clusters in Water Vapors. 1. Intermolecular Interactions. *Colloid J.* **2010**, *72*, 93−106.
(38) Zidi, Z. S. On the Stability of Ion Water Clusters at Atmospheric Conditions: Open System Monte Carlo Simulation. *J. Chem. Phys.* **2012**, *137*, 124107.
(39) Galashev, A. Y. Computer Study of Absorption of Oxygen and Ozone Molecules by Water Clusters with Cl^- and Br. *Can. J. Chem.-Rev. Can. Chim.* **2011**, *89*, 524−533.
(40) Brodskaya, E.; Lyubartsev, A. P.; Laaksonen, A. Molecular Dynamics Simulations of Water Clusters with Ions at Atmospheric Conditions. *J. Chem. Phys.* **2002**, *116*, 7879−7892.
(41) Darden, T.; Pearlman, D.; Pedersen, L. G. Ionic Charging Free Energies: Spherical Versus Periodic Boundary Conditions. *J. Chem. Phys.* **1998**, *109*, 10921−10935.
(42) Kelly, C. P.; Cramer, C. J.; Truhlar, D. G. Aqueous Solvation Free Energies of Ions and Ion-Water Clusters Based on an Accurate Value for the Absolute Aqueous Solvation Free Energy of the Proton. *J. Phys. Chem. B* **2006**, *110*, 16066−16081.
(43) Tuttle, T. R.; Malaxos, S.; Coe, J. V. A New Cluster Pair Method of Determining Absolute Single Ion Solvation Energies Demonstrated in Water and Applied to Ammonia. *J. Phys. Chem. A* **2002**, *106*, 925−932.
(44) Pollard, T.; Beck, T. L. Quasichemical Analysis of the Cluster-Pair Approximation for the Thermodynamics of Proton Hydration. *J. Chem. Phys.* **2014**, *140*, 224507.
(45) Ferrenberg, A. M.; Swendsen, R. H. Optimized Monte-Carlo Data-Analysis. *Phys. Rev. Lett.* **1989**, *63*, 1195−1198.
(46) Bennett, C. H. Efficient Estimation of Free-Energy Differences from Monte-Carlo Data. *J. Comput. Phys.* **1976**, *22*, 245−268.
(47) Hansen, J. P.; McDonald, I. R. *Theory of Simple Liquids*, 3rd ed.; Academic Press: Amsterdam, 2006.
(48) Widom, B. Some Topics in Theory of Fluids. *J. Chem. Phys.* **1963**, *39*, 2808−2812.
(49) Schenter, G. K. A Quantum Statistical Mechanical Study of the Enthalpy of Formation of the Water Dimer. *J. Chem. Phys.* **1998**, *108*, 6222−6232.
(50) Stoddard, S. D. Identifying Clusters in Computer Experiments on Systems of Particles. *J. Comput. Phys.* **1978**, *27*, 291−293.
(51) Lukyanov, S. I.; Zidi, Z. S.; Shevkunov, S. Bicanonical Monte Carlo Simulation of the Structural Properties of $Cl^-(H_2O)_n$ Clusters Using Entropy Data Based Model. *J. Mol. Struct.: THEOCHEM* **2005**, *725*, 191−206.
(52) Hill, T. L. Molecular Clusters in Imperfect Gases. *J. Chem. Phys.* **1955**, *23*, 617−622.
(53) Hill, T. L. Theory of Protein Solutions 0.1. *J. Chem. Phys.* **1955**, *23*, 623−636.
(54) Pugnaloni, L. A.; Zarragoicoechea, G. J.; Vericat, F. Cluster Pair Correlation Function of Simple Fluids: Energetic Connectivity Criteria. *J. Chem. Phys.* **2006**, *125*, 194512.
(55) Skvor, J.; Nezbeda, I. Percolation Line and Response Functions in Simple Supercritical Fluids. *Mol. Phys.* **2011**, *109*, 133−139.
(56) Berendsen, H. J. C.; Grigera, J. R.; Straatsma, T. P. The Missing Term in Effective Pair Potentials. *J. Phys. Chem.* **1987**, *91*, 6269−6271.
(57) Lamoureux, G.; MacKerell, A. D.; Roux, B. A Simple Polarizable Model of Water Based on Classical Drude Oscillators. *J. Chem. Phys.* **2003**, *119*, 5185−5197.
(58) Kiss, P. T.; Baranyai, A. A Systematic Development of a Polarizable Potential of Water. *J. Chem. Phys.* **2013**, *138*, 204507.
(59) Kiss, P. T.; Baranyai, A. A New Polarizable Force Field for Alkali and Halide Ions. *J. Chem. Phys.* **2014**, *141*, 114501.
(60) Norman, G. E.; Filinov, V. S. Investigations of Phase Transitions by a Monte-Carlo Method. *High Temp.* **1969**, *7*, 216−222.
(61) Moucka, F.; Nezbeda, I.; Smith, W. R. Computationally Efficient Monte Carlo Simulations for Polarisable Models: Multi-Particle Move Method for Water and Aqueous Electrolytes. *Mol. Simul.* **2013**, *39*, 1125−1134.

DOI: 10.1021/jp509401d
J. Phys. Chem. A 2015, 119, 488−500

(62) Paesani, F.; Iuchi, S.; Voth, G. A. Quantum Effects in Liquid Water from an Ab Initio-Based Polarizable Force Field. *J. Chem. Phys.* **2007**, *127*, 074506.
(63) Chai, J. D.; Head-Gordon, M. Long-Range Corrected Hybrid Density Functionals with Damped Atom-Atom Dispersion Corrections. *Phys. Chem. Chem. Phys.* **2008**, *10*, 6615−6620.
(64) Leverentz, H. R.; Qi, H. W.; Truhlar, D. G. Assessing the Accuracy of Density Functional and Semiempirical Wave Function Methods for Water Nanoparticles: Comparing Binding and Relative Energies of $(H_2O)_{16}$ and $(H_2O)_{17}$ to CCSD(T) Results. *J. Chem. Theory Comput.* **2013**, *9*, 995−1006.
(65) Dunning, T. H. Gaussian-Basis Sets for Use in Correlated Molecular Calculations 0.1. The Atoms Boron through Neon and Hydrogen. *J. Chem. Phys.* **1989**, *90*, 1007−1023.
(66) Frisch, M. J.; Trucks, G. W.; Schlegel, H. B.; Scuseria, G. E.; Robb, M. A.; Cheeseman, J. R.; Scalmani, G.; Barone, V.; Mennucci, B.; Petersson, G. A.; et al. *Gaussian 09*; Gaussian, Inc.: Wallingford, CT, USA, 2009.
(67) Gelb, L. D. Monte Carlo Simulations Using Sampling from an Approximate Potential. *J. Chem. Phys.* **2003**, *118*, 7747−7750.
(68) Toukan, K.; Rahman, A. Molecular-Dynamics Study of Atomic Motions in Water. *Phys. Rev. B* **1985**, *31*, 2643−2648.
(69) Lee, S. H.; Rasaiah, J. C. Molecular Dynamics Simulation of Ion Mobility 0.2. Alkali Metal and Halide Ions Using the SPC/E Model for Water at 25 Degrees C. *J. Phys. Chem.* **1996**, *100*, 1420−1425.
(70) Kell, G. S.; McLaurin, G. E. Viral Coefficients of Methanol from 150 to 300 Degrees C and Polymerization in Vapor. *J. Chem. Phys.* **1969**, *51*, 4345−4352.
(71) Kell, G. S.; McLaurin, G. E.; Whalley, E. Pvt Properties of Water 0.2. Virial Coefficients in Range 150 Degrees - 453 Degrees C without Independent Measurement of Vapor Volumes. *J. Chem. Phys.* **1968**, *48*, 3805−3813.
(72) Coe, J. V. Connecting Cluster Ions and Bulk Aqueous Solvation - a New Determination of Bulk Single-Ion Solvation Enthalpies. *Chem. Phys. Lett.* **1994**, *229*, 161−168.
(73) Buffey, I. P.; Brown, W. B. Structure of Water Clusters Computed with the Aid of Molecular Graphics. *Chem. Phys. Lett.* **1984**, *109*, 59−65.
(74) Shields, R. M.; Temelso, B.; Archer, K. A.; Morrell, T. E.; Shields, G. C. Accurate Predictions of Water Cluster Formation, $(H_2O)_{n=2-10}$. *J. Phys. Chem. A* **2010**, *114*, 11725−11737.
(75) Kiss, P. T.; Baranyai, A. Clusters of Classical Water Models. *J. Chem. Phys.* **2009**, *131*, 204310.
(76) Luo, Y.-R. *Comprehensive Handbook of Chemical Bond Energies*; CRC Press: Boca Raton, FL, 2007.
(77) Habershon, S. Zero-Point Energy Effects in Anion Solvation Shells. *Phys. Chem. Chem. Phys.* **2014**, *16*, 9154−9160.
(78) Soniat, M.; Rick, S. W. The Effects of Charge Transfer on the Aqueous Solvation of Ions. *J. Chem. Phys.* **2012**, *137*, 044511.
(79) Arshadi, M.; Yamdagni, R.; Kebarle, P. Hydration of Halide Negative Ions in Gas Phase 0.2. Comparison of Hydration Energies for Alkali Positive and Halide Negative Ions. *J. Phys. Chem.* **1970**, *74*, 1475−1482.
(80) Koneshan, S.; Rasaiah, J. C.; Lynden-Bell, R. M.; Lee, S. H. Solvent Structure, Dynamics, and Ion Mobility in Aqueous Solutions at 25 Degrees C. *J. Phys. Chem. B* **1998**, *102*, 4193−4204.
(81) Dang, L. X. Mechanism and Thermodynamics of Ion Selectivity in Aqueous-Solutions of 18-Crown-6 Ether - a Molecular-Dynamics Study. *J. Am. Chem. Soc.* **1995**, *117*, 6954−6960.
(82) Berendsen, H. J. C.; Postma, J. P. M.; van Gunsteren, W. F.; Hermans, J. In *Intermolecular Forces*; Pullman, B., Ed.; Reidel: Dordrecht, The Netherlands, 1981.
(83) Rajamani, S.; Ghosh, T.; Garde, S. Size Dependent Ion Hydration, Its Asymmetry, and Convergence to Macroscopic Behavior. *J. Chem. Phys.* **2004**, *120*, 4457−4466.
(84) Gora, R. W.; Roszak, S.; Leszczynski, J. Properties and Nature of Interactions in $Cl^-(H_2O)_n$ n=1,6 Clusters: A Theoretical Study. *Chem. Phys. Lett.* **2000**, *325*, 7−14.
(85) Xantheas, S. S. Quantitative Description of Hydrogen Bonding in Chloride-Water Clusters. *J. Phys. Chem.* **1996**, *100*, 9703−9713.

DOI: 10.1021/jp509401d
J. Phys. Chem. A 2015, 119, 488−500